

# Fabrication and Characterization of Ultralong Ag/C Nanocables, Carbonaceous Nanotubes, and Chainlike $\beta$ -Ag<sub>2</sub>Se Nanorods inside Carbonaceous Nanotubes

Dekun Ma, Meng Zhang, Guangcheng Xi, Junhao Zhang, and Yitai Qian\*

Hefei National Laboratory for Physical Sciences at Microscale, Department of Chemistry, University of Science and Technology of China, Hefei 230026, Anhui, People's Republic of China

Received January 21, 2006

A novel complex-assisted hydrothermal route is presented to fabricate ultralong Ag/C nanocables with length ranging from 100 to 180  $\mu\text{m}$  on a large scale, based on the reaction of sulfamic acid silver and salicylic acid. By chemical etching of these Ag/C nanocables, high-quality carbonaceous nanotubes can be obtained at room temperature. Using the as-prepared Ag/C nanocables as templates, a new strategy for introducing guest materials into hollow nanotubes is addressed. We take Ag<sub>2</sub>Se as an example and validate the feasibility of this strategy. All of the products are characterized in detail by multiform techniques: X-ray diffraction, Fourier transform IR, energy-dispersive X-ray analysis, field emission scanning electron microscopy, transmission electron microscopy (TEM), and high-resolution TEM. The formation mechanisms of these products are tentatively proposed.

## Introduction

One-dimensional (1D) nanostructures of metals have drawn considerable attention because of their unique physical properties and potential applications in fabricating nanoscale electronic devices as both interconnectors and active components.<sup>1</sup> Among all metals, Ag exhibits the highest thermal and electrical conductivity and has been extensively used in catalysis, electronics, photonics, photography, biological labeling, and surface-enhanced Raman scattering.<sup>2</sup> When Ag takes on a 1D nanostructure, its performance in many aspects could be potentially enhanced. The use of Ag nanowires with a higher aspect ratio loaded in polymeric composites can also significantly reduce the consumption of Ag compared with the use of Ag nanoparticles.<sup>3</sup> Therefore, many methods

have been developed to fabricate 1D Ag nanostructures,<sup>4</sup> such as an electrochemical technique, templates, poly(vinylpyrrolidone) (PVP)-directed synthesis, wet-chemical seedless and surfactantless approaches, and a hydrothermal process. However, Ag nanowires are easily corroded and tarnished upon exposure to several gaseous S-containing compounds because of its high chemical reactivity, resulting from high aspect and surface-to-volume ratios.<sup>5</sup> One solution to the problem is to coat them with an inert protective sheath.<sup>6</sup> On the other hand, metal, semiconductor, and conducting polymer nanowires sheathed by an insulative outer layer with diameters on the nanometer scale may sever as potential building blocks in various nanodevices. They are usually called nanocables. Recently, these coaxial nanocables, as a kind of new nanostructure, has been a significant issue for enhanced properties and a more diverse range of applications. A number of approaches, such as laser ablation, thermal

\* To whom correspondence should be addressed. E-mail: ytqian@ustc.edu.cn.

- (1) Xia, Y. N.; Yang, P. D.; Sun, Y. G.; Wu, Y. Y.; Mayers, B.; Gates, B.; Yin, Y. D.; Kim, F.; Yan, H. Q. *Adv. Mater.* **2003**, *15*, 53.
- (2) (a) Pestryakov, A. N.; Bogdanchikova, N. E.; Knop-Gericke, A. *Catal. Today* **2004**, *91–92*, 49. (b) Challener, W. A.; Ollmann, R. R.; Kam, K. K. *Sens. Actuators, B* **1999**, *56*, 254. (c) Jin, R. C.; Cao, Y. W.; Mirkin, C. A.; Kelly, K. L.; Schatz, G. C.; Zheng, J. G. *Science* **2001**, *294*, 1901. (d) Gould, R.; Lenhard, J. R.; Muentner, A. A.; Godlesik, S. A.; Farid, S. *J. Am. Chem. Soc.* **2000**, *122*, 1934. (e) Stoermer, R. L.; Siooss, J. A.; Keating, C. D. *Chem. Mater.* **2005**, *17*, 4356. (f) Freeman, R. G.; Grabar, K. C.; Allison, K. J.; Bright, R. M.; Davis, J. A.; Guthrie, A. P.; Hommer, M. B. M.; Jackson, A. P.; Smith, C. D.; Walter, G. M.; Natan, J. *Science* **1995**, *267*, 1629.
- (3) Sun, Y. G.; Gates, B.; Mayers, B.; Xia, Y. N. *Nano Lett.* **2002**, *2*, 165.

- (4) (a) Zhou, Y.; Yu, S. H.; Cui, X. P. C.; Wang, Y. Z.; Chen, Y. *Chem. Mater.* **1999**, *11*, 545. (b) Huang, M. H.; Choudrey, A.; Yang, P. D. *Chem. Commun.* **2000**, *12*, 1063. (c) Sun, Y. G.; Yin, Y. D.; Mayers, B. T.; Herricks, T.; Xia, Y. N. *Chem. Mater.* **2002**, *14*, 4736. (d) Caswell, K. K.; Bender, C. M.; Murphy, C. J. *Nano Lett.* **2003**, *3*, 667. (e) Wang, Z. H.; Liu, J. W.; Chen, X. Y.; Wan, J. X.; Qian, Y. T. *Chem.—Eur. J.* **2004**, *11*, 160.
- (5) (a) Graedel, T. E.; Franey, J. P.; Gualtieri, G. J.; Kammlott, G. W.; Malm, D. L. *Corros. Sci.* **1985**, *25*, 1163. (b) Elechiguerra, J. L.; Larios-Lopez, L.; Liu, C.; Garcia-Gutierrez, D.; Camacho-Bragado, A.; Yacamán, M. *J. Chem. Mater.* **2005**, *17*, 6042.
- (6) Zhu, Y. C.; Bando, Y.; Yin, L. W. *Adv. Mater.* **2004**, *16*, 331.

evaporation,  $\gamma$  irradiation, and templating, have been developed to fabricate these kinds of coaxial 1D nanostructures.<sup>7</sup>

The study of Ag nanocables has attracted much attention. For instance, Ag/cross-linked poly(vinyl alcohol) (PVA) nanocables could be fabricated by using polymer PVA as a reducer and bond under hydrothermal process conditions.<sup>8</sup> Through a redox reaction between silver nitrite and pyrrole with PVP as an assistant agent, Ag/pyrrole nanocables have been obtained.<sup>9</sup> Adopting a hydrothermal or microwave-assisted hydrothermal reduction/carbonization process with starch or sucrose as the carbon source and reducer, Ag/C nanocables with lengths ranging from 1 to 10  $\mu\text{m}$  could be synthesized.<sup>10</sup> In this paper, we report a novel complex-assisted hydrothermal route to fabricate ultralong Ag/C nanocables with lengths ranging from 100 to 180  $\mu\text{m}$ , based on the reaction of the complex of sulfamic acid silver and salicylic acid.

1D tubular nanostructures are an interesting and increasingly important class of materials with diverse applications, ranging from drug delivery, cell and enzyme transplantation, filtration and purification applications, and gene therapy.<sup>11</sup> They also can be used as nanocargo and nanoreactors because of their inner cavity.<sup>12</sup> Although various kinds of nanotubes have been prepared, such as inorganic nanotubes, organic nanotubes, and biological nanotubes, the fabrication of novel ultralong nanotubes is still desirable.<sup>1,13</sup>

Herein, we fabricated ultralong carbonaceous nanotubes by etching as-prepared Ag/C nanocables with a solution of KCN at room temperature. To the best of our knowledge, there have been few reports on ultralong amorphous carbonaceous nanotubes (>100  $\mu\text{m}$ ) at present.

Impregnation of hollow tubes with guest materials provides a potentially fascinating route to prepare functional nanomaterials for a variety of applications.<sup>14</sup> In this regard, carbon nanotubes have become the focus of study. For example,

ionic species, organic molecules, metals, and oxides has been successfully introduced into carbon nanotubes.<sup>14b,15</sup> The mechanism of encapsulation is simple: using capillary action, guest materials are diffused into carbon nanotubes, remaining inside the tubes and aligning one-dimensionally.<sup>16</sup> Distinct from carbon nanotubes, organic and biological nanotubes can incorporate guest materials by their tunable interior chemical functional groups.<sup>14e,17</sup> In this report, we present a novel approach to the introduction of guest materials into carbonaceous nanotubes, which is different from the above-mentioned mechanism. We use as-prepared Ag/C nanocables as templates, and guest materials can be introduced into carbonaceous nanotubes by chemical reaction with Ag cores. An example for introducing  $\text{Ag}_2\text{Se}$  into carbonaceous nanotubes was taken, and this kind of encapsulation structure was also characterized in detail.

## Experimental Section

**Fabrication of Ultralong Ag/C Nanocables.** A total of 0.001 mol of  $\text{AgNO}_3$  was dissolved in 45 mL of distilled water. Then 0.0005 mol of  $\text{K}_2\text{CO}_3$  was put into the solution. Immediately, a quantity of milk-white precipitation formed. Subsequently, 0.002 mol of  $\text{NH}_2\text{SO}_3\text{H}$  was added into the above solution with stirring. The milk-white precipitation was promptly dissolved, and the solution became transparent. The transparent solution was stirred for a while, and then 0.002 mol of salicylic acid was put into it. After agitation for several minutes, the solution was poured into a stainless steel autoclave with a Teflon liner of 60-mL capability and heated at 200  $^\circ\text{C}$  for 36 h. After the autoclave was cooled to room temperature, the resulting gray fluffy floater was separated centrifugally and washed with distilled water and then absolute ethanol three times. Then the products were dried under vacuum at 60  $^\circ\text{C}$  for 4 h.

**Fabrication of Carbonaceous Nanotubes.** A total of 0.017 g of Ag/C nanocables was dispersed into 40 mL of distilled water. Then 0.13 g of KCN was put into the solution. The solution was left to sit for 24 h, after which it was centrifuged to isolate the precipitate that contained the hollow nanotubes. The precipitates were washed by distilled water and absolute ethanol three times. Then the products were dried under vacuum at 60  $^\circ\text{C}$  for further characterization.

**Fabrication of Single-Crystalline Chainlike  $\beta\text{-Ag}_2\text{Se}$  Nanorods Encapsulated inside Carbonaceous Nanotubes.** A total of 0.034 g of Ag/C nanocables was first dispersed into 35 mL of distilled water by agitation. Subsequently, 10 mL of  $\text{N}_2\text{H}_4\cdot\text{H}_2\text{O}$  was decanted into the solution. Then, 0.078 g of Se powder was joined to the solution. After the solution was stirred for a while, it was put into a stainless steel autoclave with a Teflon liner of 60-mL capability, sealed, and heated at 180  $^\circ\text{C}$  for 12 h. After the autoclave was cooled to room temperature, the products were separated centrifugally and washed with a dilute solution of KCN, distilled water, and absolute ethanol three times. Then the products were dried under vacuum at 50  $^\circ\text{C}$  for 4 h.

- (7) (a) Zhang, Y.; Suenaga, K.; Colliex, C.; Iijima, S. *Science* **1998**, *28*, 973. (b) Hu, J. Q.; Bando, Y.; Liu, Z. W.; Sekiguchi, T.; Golberg, D.; Zhan, J. H. *J. Am. Chem. Soc.* **2003**, *125*, 11306. (c) Xie, Y.; Qiao, Z. P.; Chen, M.; Liu, X. M.; Qian, Y. T. *Adv. Mater.* **1999**, *11*, 1512. (d) Jiang, X. C.; Mayers, B.; Herricks, T.; Xia, Y. N. *Adv. Mater.* **2003**, *15*, 1740.
- (8) Luo, L. B.; Yu, S. H.; Qian, H. S.; Zhou, T. *J. Am. Chem. Soc.* **2005**, *127*, 2822.
- (9) Chen, A. H.; Wang, H. Q.; Li, X. Y. *Chem. Commun.* **2005**, *14*, 1863.
- (10) (a) Yu, J. C.; Hu, X. L.; Quan, L. B.; Zhang, L. Z. *Chem. Commun.* **2005**, *21*, 2704. (b) Yu, S. H.; Cui, X. J.; Li, L. L.; Li, K.; Yu, B.; Antonietti, M.; Colfen, H. *Adv. Mater.* **2004**, *16*, 1636.
- (11) (a) Langer, R. *Science* **1990**, *249*, 1527. (b) Gill, I.; Ballesteros, A. J. *Am. Chem. Soc.* **1998**, *120*, 8587. (c) Schnur, J. M.; Pice, R.; Rudolph, A. S. *J. Controlled Release* **1994**, *28*, 3. (d) Kmiec, E. B. *Am. Sci.* **1999**, *87*, 240.
- (12) (a) Han, W. Q.; Kohler-Redlich, P.; Scheu, C.; Ernst, F.; Ruhle, M.; Grobert, N.; Terrones, M.; Kroto, H. W.; Walton, D. R. M. *Adv. Mater.* **2000**, *12*, 1356. (b) Pham, H. C.; Keller, N.; Estournes, C.; Ehret, G.; Greneche, J. M.; Ledoux, M. J. *Phys. Chem. Chem. Phys.* **2003**, *5*, 3716.
- (13) Shimizu, T.; Masuda, M.; Minamikawa, H. *Chem. Rev.* **2005**, *105*, 1401.
- (14) (a) Ajayan, P. M.; Iijima, S. *Nature* **1993**, *361*, 333. (b) Gao, Y.; Bando, Y. *Nature* **2002**, *415*, 599. (c) Lee, J.; Kim, H.; Kahng, S. J.; Kim, G.; Son, Y. W.; Ihm, J.; Kato, H.; Wang, Z. W.; Okazaki, T.; Shinohara, H.; Kuk, Y. *Nature* **2002**, *415*, 1005. (d) Dujardin, E.; Peet, C.; Stubbs, G.; Culver, J. N.; Mann, S. *Nano. Lett.* **2003**, *3*, 413. (e) Wang, X. S.; Wang, H.; Coombs, N.; Winnik, M. A.; Manners, I. *J. Am. Chem. Soc.* **2005**, *127*, 8924.

- (15) (a) Meyer, R. R.; Sloan, J.; Dunin-Borkowski, R. E.; Kirkland, A. I.; Novotny, M. C.; Bailey, S. R.; Hutchison, J. L.; Green, H. *Science* **2000**, *289*, 1324. (b) Takenobu, T.; Takano, T.; Shiraiishi, M.; Murakami, Y.; Ata, M.; Kataura, H.; Iwasa, Y. Y. *Nat. Mater.* **2003**, *2*, 683. (c) Yuge, R.; Ichihashi, T.; Shimakawa, Y.; Kubo, Y.; Yudasaka, M.; Iijima, S. *Adv. Mater.* **2004**, *16*, 1420.
- (16) Guerretpiecourt, C.; Lebouar, Loiseau, Y. A.; Pascard, H. *Nature* **1994**, *372*, 761.
- (17) Yan, X. H.; Liu, G. J.; Liu, F. T.; Tang, B. Z.; Peng, H.; Pakhomov, A. B.; Wong, C. Y. *Angew. Chem., Int. Ed.* **2001**, *40*, 3593.

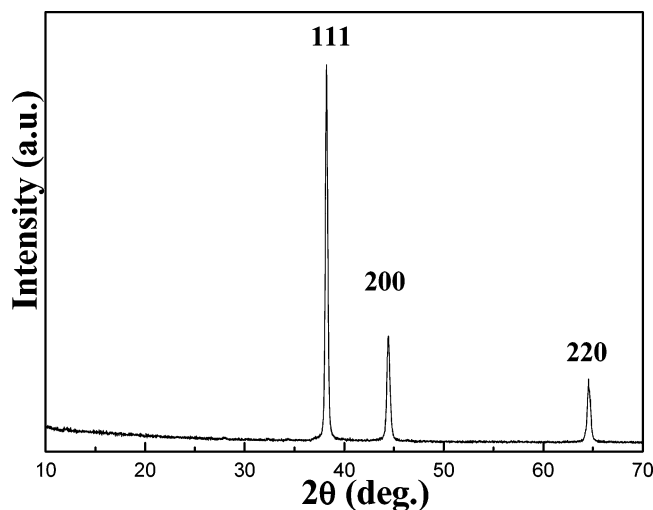


**Figure 1.** XRD pattern of the nanocables obtained at 200 °C for 36 h.

**Characterization.** X-ray diffraction (XRD) patterns were carried out with a Philips X'Pert PRO SUPER X-ray diffractometer equipped with graphite-monochromatized Cu K $\alpha$  radiation ( $\lambda = 1.541\ 874\ \text{\AA}$ ) in the  $2\theta$  range from 10° to 70°. IR spectra were obtained on a Bruker Vector-22 Fourier transform IR (FTIR) spectrometer from 4000 to 500  $\text{cm}^{-1}$  at room temperature. The samples and KBr crystal were ground together, and the mixture was pressed into a flake for IR spectroscopy. Field emission scanning electron microscopy (FE-SEM) images were taken on a JEOL JSM-6700 scanning electron microscope. The transmission electron microscopy (TEM) images were performed on a Hitachi model H-800 instrument with a tungsten filament, using an accelerating voltage of 200 kV. High-resolution TEM (HRTEM) images, selected area electronic diffraction (SAED) patterns, and energy-dispersive spectroscopy (EDS) were carried out on a JEOL 2010 transmission electron microscope at an accelerating voltage of 200 kV.

## Results and Discussion

**Characterization of Ag/C Nanocables.** Silver nitrate can be completely changed into Ag/C nanocables, and the yield of Ag/C nanocables is 100%. The crystallinity and purity of phase of the products were examined by an X-ray powder diffractometer. Figure 1a shows a typical XRD pattern of the products. All of the reflections can be indexed to the face-centered-cubic phase of Ag [space group:  $Fm\bar{3}m$  (225)], which is in good agreement with the reported data ( $a = 4.086\ \text{\AA}$ , JCPDS No. 04-0783). The morphologies and microstructures of the as-prepared products were further surveyed by FE-SEM and TEM. Figure 2a shows a typical FE-SEM image of the as-prepared Ag/C nanocables. Clearly, these nanocables have diameters ranging from 100 to 160 nm and lengths ranging from 100 to 180  $\mu\text{m}$ . The calculations based on statistical 100 nanocables show that the aspect ratios of these nanocables are more than 500. Each nanocable exhibits a uniform diameter along its entire length. Figure 2b displays a bright-field TEM image of the Ag/C nanocables. The clear bright/dark contrast (see the inset, which is a magnified image of the black frame in Figure 2b) along the radial direction indicates the structure of the core-shell cable. The dark-core part corresponds to Ag, which is 120 nm in diameter.

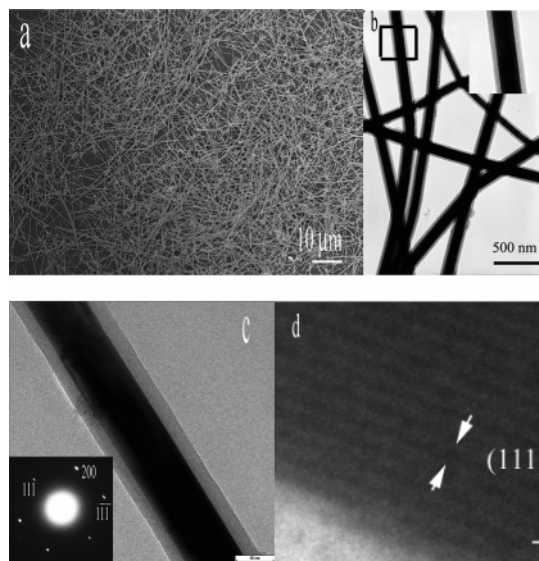


**Figure 2.** (a) FE-SEM image of the nanocables. (b) TEM image of the nanocables. Inset: magnified TEM image of the black frame. (c) TEM image of an individual nanocable. Inset: SAED pattern recorded on this nanocable. (d) HRTEM image recorded on the edge of this nanocable.

Outside of the core region, the light part corresponds to a carbonaceous shell, which is 40 nm in diameter. A typical EDX spectrum taken from a single nanocable also confirms that the nanocable is composed of only an Ag core and a carbonaceous shell (see Supporting Information Figure S1). HRTEM and SAED patterns are further used to characterize the as-prepared nanocables. Figure 2c is a bright-field TEM image of an individual Ag/C nanocable. The SAED pattern indicates the single-crystalline nature of the Ag core. Figure 2d is a HRTEM image taken from the edge of this nanocable. The spacing of the adjacent lattice plane is 2.36  $\text{\AA}$ , which is consistent with the separation of Ag{111} planes.

**Reaction Mechanisms or the Formation Process of Ag/C Nanocables.** The fresh Ag<sub>2</sub>CO<sub>3</sub> deposition can be dissolved by sulfamic acid and form sulfamic acid silver.<sup>18</sup> This complex can limit the concentration of free Ag ions in solution. Salicylic acid, as a weak reducer, can reduce Ag ions under hydrothermal conditions. The default experiments in the absence of salicylic acid showed that no Ag was produced, which confirmed the role of salicylic acid as a reducer. In place of salicylic acid with NaBH<sub>4</sub>, a strong reducer, keeping other conditions constant, only irregular particles were obtained (data not shown here). In addition, when we used AgNO<sub>3</sub> instead of sulfamic acid silver, we only obtained a few nanowires. Therefore, a relatively low concentration of free Ag ions in solution and a weak reducer adjusted the rate of nucleation and growth well, which was favorable to the formation of ultralong Ag/C nanocables. The temperature also played an important role in fabricating ultralong Ag/C nanocables. If the reaction temperature was lower than 120 °C, no solid Ag was observed. If the temperature was lower than 160 °C or more than 220 °C, high-quality Ag/C nanocables could not be obtained.

(18) Bicbli, L.; Vecchia, L. *Ann. Chim. (Rome)* **1956**, *46*, 351.

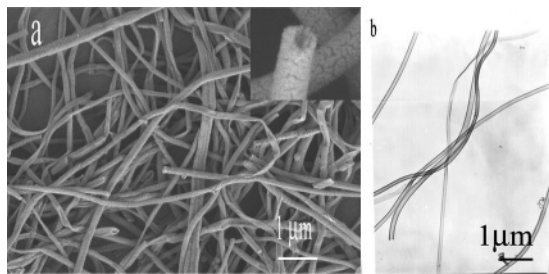


**Figure 3.** (a) FE-SEM image of carbonaceous nanotubes. Inset: magnified FE-SEM image. (b) TEM image of carbonaceous nanotubes.

To investigate the formation process of Ag/C nanocables, time-dependent TEM observation has been carried out (see Supporting Information Figure S2). At initial 4 h, the products were all particles. When the time of hydrothermal growth was prolonged to 12 h, only a few nanocables were produced. Evidently, a large number of nanocables formed if the time was prolonged to 24 h. However, there were still some nanoparticles in the products. After the hydrothermal growth had proceeded for 36 h, the products were almost all nanocables. The Ostwald ripening process has been most frequently used to explain for the growth of 1D nanostructures of metal in solution.<sup>4c,19</sup> On the basis of the above-mentioned TEM observation, the growth of Ag/C nanocables was believed to follow a similar process. Ag nanoparticles could grow continuously into uniform Ag nanowires at the expense of smaller ones through this ripening mechanism. We also observed that Ag nanoparticles were coated by an organic substance in the growth process (see Supporting Information Figure S2a). Possibly, the selective adsorption of organic molecules on some crystalline faces of Ag particles led to the preferential growth of the other crystalline faces. Ag nanoparticles eventually grew into 1D nanowires, and organic molecules outside of the Ag nanowires were carbonized because of a long-playing hydrothermal process.

**Characterization and Discussion of Carbonaceous Nanotubes.** By chemical etching, large numbers of amorphous carbonaceous nanotubes can be obtained from Ag/C nanocables. The yield of carbonaceous nanotubes is 100%. Ag can be dissolved by the solution of KCN and forms  $\text{Ag}(\text{CN})_2^-$ . Because the tips of the nanocables are open (see Supporting Information Figure S3),  $\text{CN}^-$  ions and  $\text{O}_2$  molecules can easily be diffused into nanocables. With longer time diffusion and dissolution process, the Ag core can be completely consumed (see Supporting Information Figure S4). Because this etching is operated at room temperature, these carbonaceous nanotubes keep the original frame of the Ag/C nanocables. Figure 3a shows a FE-SEM image of the products. These nanotubes keep the initial size and the shape of nanocables well. The tips of the nanotubes are open, as the inset in Figure 3a shows. In Figure 3b, the TEM image further displays these kinds of tubular nanostructures more clearly. FTIR spectroscopy (see Supporting Information Figure S5) of the nanotubes indicates that only some hydroxyl groups and carbonyl groups are present, which

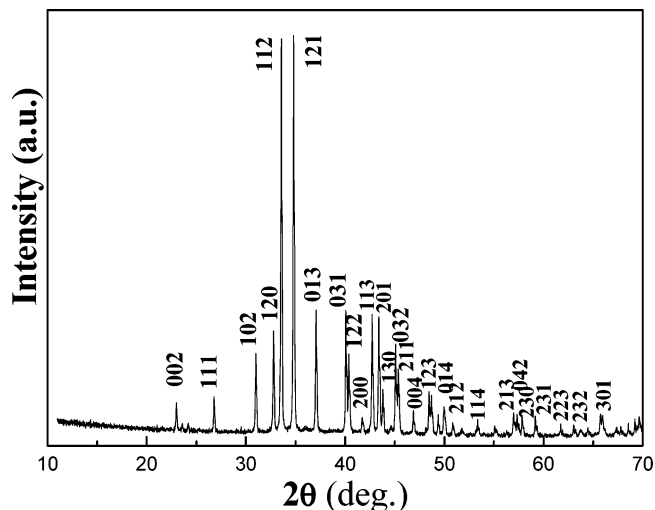


**Figure 4.** XRD pattern of products prepared by using Ag/C nanocables as templates.

might be the result of carbonization of the organic compound.<sup>20</sup>

**Characterization and Discussion of  $\beta$ -Ag<sub>2</sub>Se Nanorods inside Carbonaceous Nanotubes.** Encapsulation of chainlike  $\beta$ -Ag<sub>2</sub>Se nanorods inside carbonaceous nanotubes could be obtained from the reaction of Se with Ag/C nanocables at the assistance of  $\text{N}_2\text{H}_4\cdot\text{H}_2\text{O}$ . The yield of  $\beta$ -Ag<sub>2</sub>Se nanorods inside carbonaceous nanotubes can be more than 98%.

Furthermore, this method could be used to prepare other Ag-containing compounds inside carbonaceous nanotubes (see Supporting Information Figure S6). Here, we take Ag<sub>2</sub>Se as an example for detailed study.

Figure 4a shows the XRD pattern of as-prepared products, which can be indexed to a pure orthorhombic  $\beta$ -Ag<sub>2</sub>Se phase. The calculated lattice constants from the XRD pattern are  $a = 4.326 \text{ \AA}$ ,  $b = 7.017 \text{ \AA}$ , and  $c = 7.748 \text{ \AA}$ , which are in agreement with the reported values (JCPDS No. 24-1041). Figure 5a shows the TEM image of as-synthesized  $\beta$ -Ag<sub>2</sub>Se nanorods encapsulated in carbonaceous nanotubes. The products keep the lengths of the Ag/C nanocable templates ranging from 100 to 180  $\mu\text{m}$ . The bright/dark contrast along the radial direction indicates the core-shell structure. Figure 5b exhibits a magnified TEM image of an individual Ag<sub>2</sub>Se nanorod encapsulated inside carbonaceous nanotubes. EDS (see Supporting Information Figure S7) recorded on this Ag<sub>2</sub>Se nanorod at the middle position proved that the product chiefly consists of Ag, Se, and a small quantity of C and O. EDS data show that the ratio of Ag to Se is 66.10:33.90, which is very close to 2:1. The SAED pattern that was recorded from this nanorod indicated its single-crystalline nature. Figure 5c shows a HRTEM image taken from the edge of the Ag<sub>2</sub>Se nanorod. The spacing of the adjacent lattice plane is ca. 2.89  $\text{\AA}$ , which is consistent with the interplanar spacing of Ag<sub>2</sub>Se (102) planes. It also demonstrated that the nanorod was well-crystallized. Further studies of both the HRTEM and SAED patterns show that the axial growth plane is (102) and the growth direction is [001].

(19) Sun, Y. G.; Mayers, B.; Herricks, T.; Xia, Y. N. *Nano Lett.* **2003**, *3*, 955.

(20) Sun, X. M.; Li, Y. D. *Adv. Mater.* **2005**, *17*, 2626.

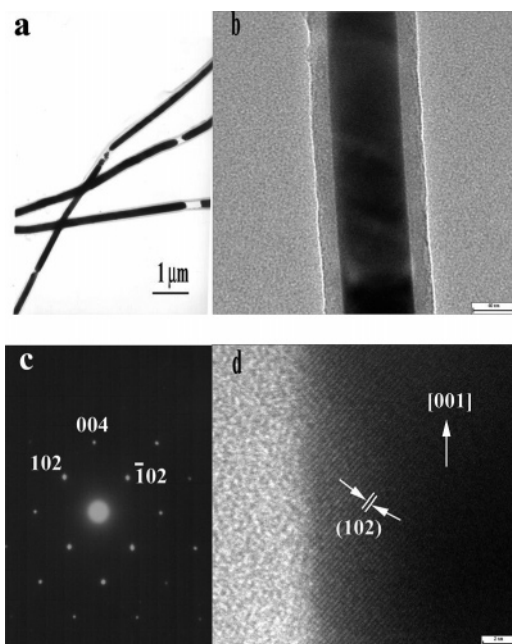


**Figure 5.** (a) TEM image of  $\beta$ -Ag<sub>2</sub>Se nanorods encapsulated in carbonaceous nanotubes. (b) TEM image of an individual magnified Ag<sub>2</sub>Se nanorod inside carbonaceous nanotubes. (c) SAED pattern recorded on this nanorod. (d) HRTEM image recorded on the edge of this nanocable.

Previously, a hydrothermal route had been reported to synthesize Ag<sub>2</sub>Se at elevated temperature (>260 °C) and pressure (100 atm).<sup>21</sup> However, at the present reaction conditions, Ag<sub>2</sub>Se could be obtained at relatively lower temperature and pressure. The default experiments in the absence of N<sub>2</sub>H<sub>4</sub>·H<sub>2</sub>O showed that there were many unreacted Ag ions in the products. According to a previous report, hydrazine often acts as the coordinating agent, electron transfer, and reducing agent to synthesize various metal chalcogenides.<sup>22</sup> Possibly, in our reaction system, Se was first reduced to Se<sup>2-</sup> ions by hydrazine, which more easily reacted with Ag. On the other hand, hydrazine possibly played a role of electron transfer, which precipitated the reaction.

To the syntheses of Ag<sub>2</sub>Se nanocrystals by a templating approach, a previous study showed that crystallinity of Ag<sub>2</sub>Se depended on the choice of the solid templates: single-crystalline Ag<sub>2</sub>Se nanowires were formed from a Se template, while polycrystalline Ag<sub>2</sub>Se nanotubes from a Ag template.<sup>41</sup> For Se nanowire templates, the Ag ions were introduced outside of the nanowires and diffused inward through the entire template. The Se ions do not have to move as much, and single crystallinity of each template is essentially preserved. As for Ag nanowire templates, conversely, it is the Ag template material itself that migrates outward to contact with the Se colloid and form a Ag<sub>2</sub>Se solid. Silver selenide, in this case, nucleates simultaneously at the multiple

contact points along the longitudinal axis of each Ag nanowire. As a result, the polycrystalline Ag<sub>2</sub>Se nanowires were obtained. Therefore, a question arises here: why did we obtain single-crystalline Ag<sub>2</sub>Se nanorods when we used Ag nanowires encapsulated inside carbonaceous nanotubes as templates? Although the exact reasons for the formation of single-crystalline Ag<sub>2</sub>Se nanorods through this method are unclear at present, we believe the following: (1) Se could react with hydrazine and form Se<sup>2-</sup> ions, which are more easily diffused inward through the entire Ag nanowire than the Se colloid. (2) The carbonaceous shells constrained the migration of Ag nanowire templates. The nucleation and growth of Ag<sub>2</sub>Se occurred in a confined space, which benefits the formation of single-crystalline nanorods. Then, a subsequent question is as follows: why did we not gain entire nanowires but chainlike nanorods? A possible explanation for this is as follows: the difference of the structures and lattice constants between Ag and Ag<sub>2</sub>Se will cause the reorganization of Ag atoms in the solid templates. The reorganization maybe results in stress. When the stress is accumulated to a certain extent, it will be released through the rupture of Ag nanowires. As a result, chainlike Ag<sub>2</sub>Se nanorods are produced and arranged along the axial direction of carbonaceous nanotubes. To know clearly the formation mechanism of single-crystalline chainlike  $\beta$ -Ag<sub>2</sub>Se nanorods encapsulated inside carbonaceous nanotubes, a further study of this issue has been underway.

## Conclusion

We have successfully fabricated ultralong Ag/C nanocables via a complex-assisted hydrothermal route at 200 °C for 36 h. The complex function of sulfamic acid and the role of a weak reducer of salicylic acid benefitted the obtainment of Ag/C nanocables. By removing the Ag core, we obtained high-quality carbonaceous nanotubes. These carbonaceous nanotubes kept the same lengths of Ag/C nanocables and sizes of the shell. Single-crystalline chainlike  $\beta$ -Ag<sub>2</sub>Se nanorods could be encapsulated inside carbonaceous nanotubes using the as-prepared Ag/C nanocables as templates. The easy diffusion of Se<sup>2-</sup> ions through the entire Ag nanowires and the restrictive effect of carbonaceous shells were attributed to the formation of single-crystalline Ag<sub>2</sub>Se. The chainlike nanorods, not entire nanowires, possibly resulted from the stress. This new strategy for encapsulating guest materials into carbonaceous nanotubes could be extended to prepare other Ag-containing compounds, such as Ag<sub>2</sub>S and Ag<sub>2</sub>Te.

**Acknowledgment.** Financial support from the National Nature Science Fund of China and the 973 Project of China (Grant Nos. 2005CB623601).

**Supporting Information Available:** Figures of EDX and FTIR spectra and TEM images. This material is available free of charge via the Internet at <http://pubs.acs.org>.

IC0601261

(21) Cambi, L.; Elli, M. *Chim. Ind.* **1968**, *50*, 94.

(22) Li, Y. D.; Ding, Y.; Wang, Z. Y. *Adv. Mater.* **1999**, *11*, 847.

(23) Gates, B.; Mayers, B.; Wu, Y. Y.; Sun, Y. G.; Cattle, B.; Yang, P. D.; Xia, Y. N. *Adv. Funct. Mater.* **2002**, *12*, 679.